

# CLASSIFICATION OF BOTTOM-SET TARGETS FROM WIDEBAND ECHO RESPONSES TO BIO-INSPIRED SONAR PULSES

C. Capus      Ocean Systems Laboratory, Heriot-Watt University, Edinburgh, UK  
Y. Pailhas     Ocean Systems Laboratory, Heriot-Watt University, Edinburgh, UK  
K.E. Brown    Ocean Systems Laboratory, Heriot-Watt University, Edinburgh, UK

## 1 INTRODUCTION

Detection and classification of targets in sidescan and other sonar imagery is well advanced. Standard image processing techniques operate on intensity data and usually sonar returns are matched filtered to improve echo localisation and signal-to-noise ratio (SNR). These methods allow large amounts of data to be processed quickly and produce good results. Typically detection rates in excess of 90% are attainable with false alarm rates around 5%, though performance declines rapidly over heavily cluttered seabeds. To further increase effectiveness of target identification from sonar data we must find new approaches. This paper considers the contribution of detailed echo analysis using bio-inspired wideband sonar pulses.

## 2 BACKGROUND

### 2.1 Dolphin Data Analysis

The transmit signals used in this research have been derived from previous work on the analysis of bottlenose dolphin (*Tursiops truncatus*) clicks. The data came from experiments in which dolphins were performing target detection and discrimination tasks [1]. In the main the signals followed well documented patterns and could be classified using Houser's click taxonomy [2]. Spectral distributions are characteristically centred on two major regions above and below 70kHz. The first dataset analysed comprised transmit signals used to recognise differences between contents of otherwise identical aluminium flasks of approximately 100mm diameter. The experiments involved two trial types. The first tested the dolphins ability to match to a sample. The sample is presented and the dolphin is allowed to examine it from a range of 5.4m. The sample is then removed and the dolphin is required to choose a matching flask from a set of three presented at the same range. In the second type of trial there is a training period in which the dolphin can learn to recognise differences in echo response between the filled flasks. During the trial a single flask is presented and the dolphin makes a decision based on its learning. A final dataset came from a free swimming experiment in which the dolphin is required to detect and identify a target within a range of approximately 50m from a workboat.

It has been noted that dolphins require the use of high frequencies to produce the highest output intensities [3]. In the datasets analysed here, the target ranges are relatively short and both high and low frequency dominant clicks are used. In the identification task with pre-trial learning a greater proportion of wideband clicks were noted. In the match-to-sample task the dolphins used predominantly type A, unimodal low frequency, and type B, unimodal low frequency with a secondary high frequency peak within 10dB of the maximum level. In the free swimming experiment two distinct phases were noted. These seemed to correspond to a general search strategy during target detection, or when seeking the workboat and a second interrogation phase at close range to the target. During general search the clicks are typically low amplitude and predominantly low frequency. Pulse variability was higher during the interrogation phase, with mixtures of low, high and wideband clicks. Signal levels were substantially higher during this phase.

## 2.2 Bio-inspired signals

We have developed a set of six pulses based on the observations above. Each pulse is constructed from two linear chirp components which overlap both in time and frequency, see Figure 1. Full details of these signals are given elsewhere [4], but the relevant parameters for the chirp components are reproduced in Table 1.

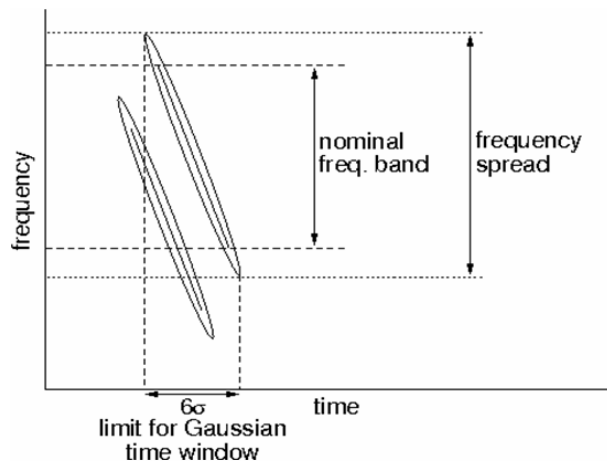


Figure 1: Chirp components for bio-inspired signals

Signal	Chirp rate, $a$ (kHzs <sup>-1</sup> )	Nominal frequency bands	
		Chirp 1	Chirp 2
DC1	$-0.420 \times 10^6$	30-114kHz	46-130kHz
DC2	$-0.375 \times 10^6$	30-105kHz	55-130kHz
DC3	$-0.330 \times 10^6$	30-96kHz	64-130kHz
DC4	$-0.300 \times 10^6$	30-90kHz	70-130kHz
DC5	$-0.270 \times 10^6$	30-84kHz	76-130kHz
DC6	$-0.240 \times 10^6$	30-78kHz	82-130kHz

Table 1: Parameters for bio-inspired signal set

## 3 ECHO VARIATION WITH SIGNAL

The returns plotted in Figure 2 demonstrate how marked the differences in response can be for minimal changes in the structure of the outgoing pulse. These are records from test tank experimentation ensonifying a small solid copper reference sphere of 23mm diameter. The target response for signal DC1 is considerably higher than the reverberation level from the concrete tank floor. Using DC2 however, the target response is reduced and the reverberation level is considerably higher. Using this pulse combination gives us some ability to switch between high returns from the target and high returns from the surroundings and may suggest one reason for pulse variability in the dolphin during target interrogation. The identification process and final decision may involve surrounding context information as well as characteristic target responses.

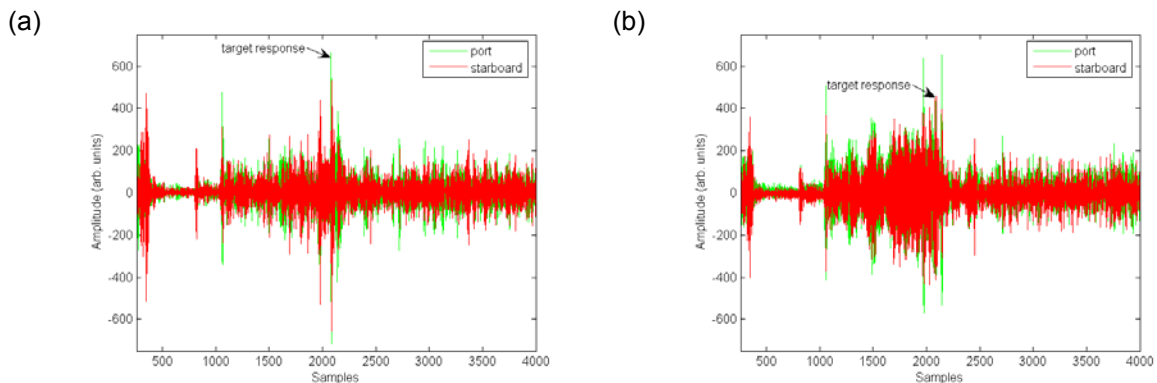


Figure 2: (a) signal DC1, high target response and relatively low reverberation level; (b) signal DC2, high reverberation level and relatively low target response. The target is a solid copper calibration sphere ( = 23mm) at ~6m range

It should be noted that the gross differences seen in the above returns can be consistently reproduced. Pulse DC2 has frequently produced noticeably different results than the majority of other signals in the set during tank experimentation.

### 3.1 Target resonances

Echoes from a small number of the test targets have displayed significant energy at the extremes of the transmit band, with certain pulse/target combinations particularly well tuned to highlighting these responses. One example is given in Figure 3 where higher than expected returns, which seem to correspond to resonant frequencies in the target, are seen at around 130-150kHz. These are well brought out both by DC1 and DC6, but for DC6 it is more pronounced with echo levels >5dB higher than expected in this region.

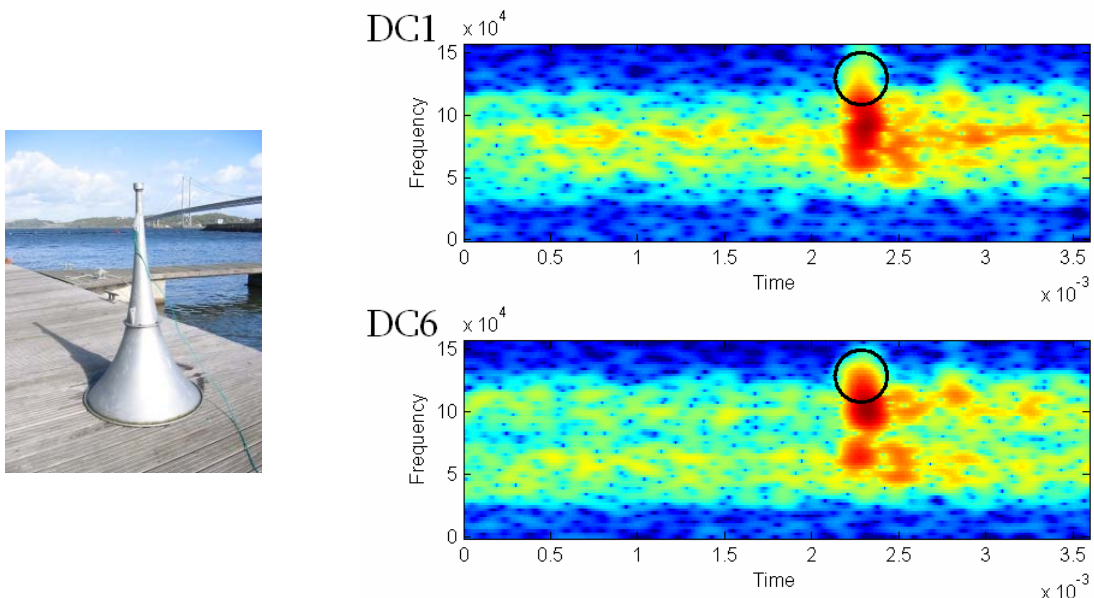


Figure 3: Spectrograms for responses of the concave cone target depicted

### 3.2 Theoretical target resonance models

Accurate models exist for the description of the detailed signal echo from simple forms, for example spherical and cylindrical objects. We have used the modal decompositions proposed by Doolittle and Uberall [5] for comparison with empirical data. Figure 4 shows the correspondence between the

theoretical and measured responses for a cylindrical PVC pipe of 170mm diameter and 3mm wall thickness.

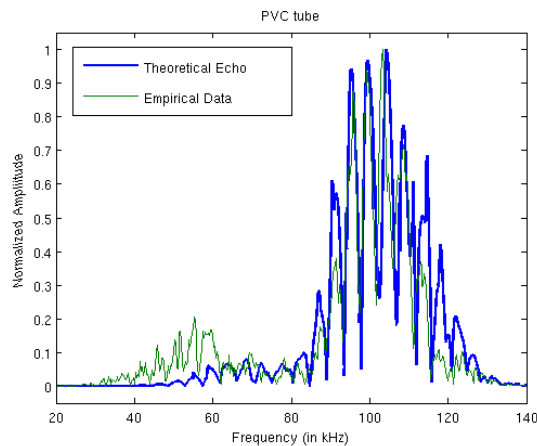


Figure 4: Theoretical target response match to empirically derived response for 170mm diameter PVC tube – reverberation dominates the empirical response below 70kHz

The theoretical response has been modified using the known transducer sensitivities. The most important aspect is the ability to accurately model the peak and notch positions to achieve an excellent match with the empirical data.

### 3.3 Bat Sonar

The use of spectral features, especially notch information, has been implicated in a number of discrimination tasks for FM bats [6-8]. Echoes with separations of less than around 500 $\mu$ s tend to be interpreted as responses from a single target. Notches arising from interferences between echo fronts arriving within this integration period are believed to provide information about target physical properties and location. The anatomical structure of the ear itself delivers multiple reflections to the auditory apparatus and these can provide target elevation information from the location of resulting notches in the spectrum [9].

## 4 CLASSIFICATION

### 4.1 Frequency resolution and integration times

For underwater sonar applications, the key characteristic features in the broadband echo spectra are also the strong peaks and notches derived from interactions between multiple echo fronts. To represent these interference patterns effectively over the  $ka$  ranges suggested above, we require around 1kHz resolution and need to integrate returns over approximately 1ms to achieve this. The spectrograms in Figure 3 illustrate this for a 100mm diameter cylindrical flask similar to that used in the dolphin experiments previously described. The target is suspended midwater at a range of approximately 20m from the sonar. The characteristic oscillatory frequency response for this target first becomes clear when the short-time window used in calculation of the spectrogram reaches 256 samples, equivalent to an 820 $\mu$ s integration time at the sampling frequency of 312.5kHz. Using longer windows the characteristic response becomes clearer. Above 1024 samples, integration time in excess of 3ms, loss of time and range resolution and reduced SNR become more of an issue. These responses indicate that it may be sensible to employ a joint approach, using short integration times for target detection and localisation while relying on longer integration times to elicit spectral information which may be used for classification and identification. Experimentally derived integration times for the bottlenose dolphin are around 260 $\mu$ s [3], but it is important to note that frequency resolution is determined by the cochlear response characteristics which will certainly extend to the 1kHz resolution required to represent the spectral content for these echoes. This integration time will also include all of the key echo fronts for this sort of target.

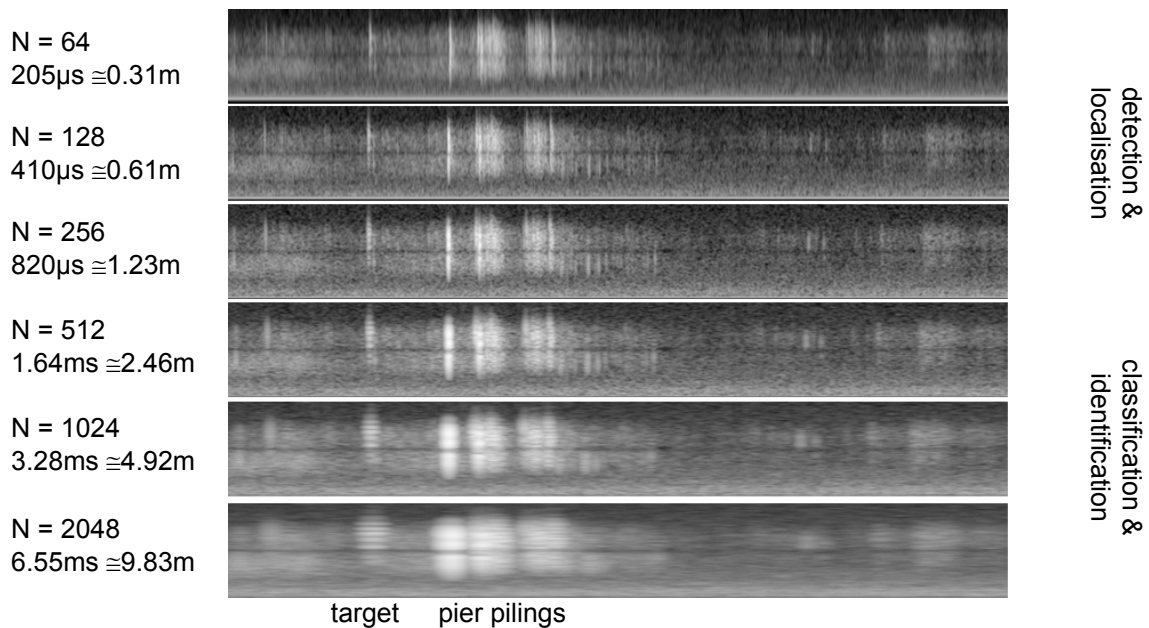


Figure 5: Spectrograms showing echo response from a cylindrical target at 20m range computed with different short time windows -- sampling frequency is 312.5kHz; left column gives window lengths with corresponding integration time and range

#### 4.2 Localisation of spectral peaks and notches

We now return to further test tank data and propose a simple method for extraction of key spectral features. The strongest features are the spectral notches, though for some targets these are still small compared to a generally high echo response across the frequency bands used. The important features can still be extracted by applying a threshold on the second derivatives of the echo spectrum. We use the threshold to output a binary spectral signature for the target.

**Cone target; signal DC6; sonar head angle 0°**

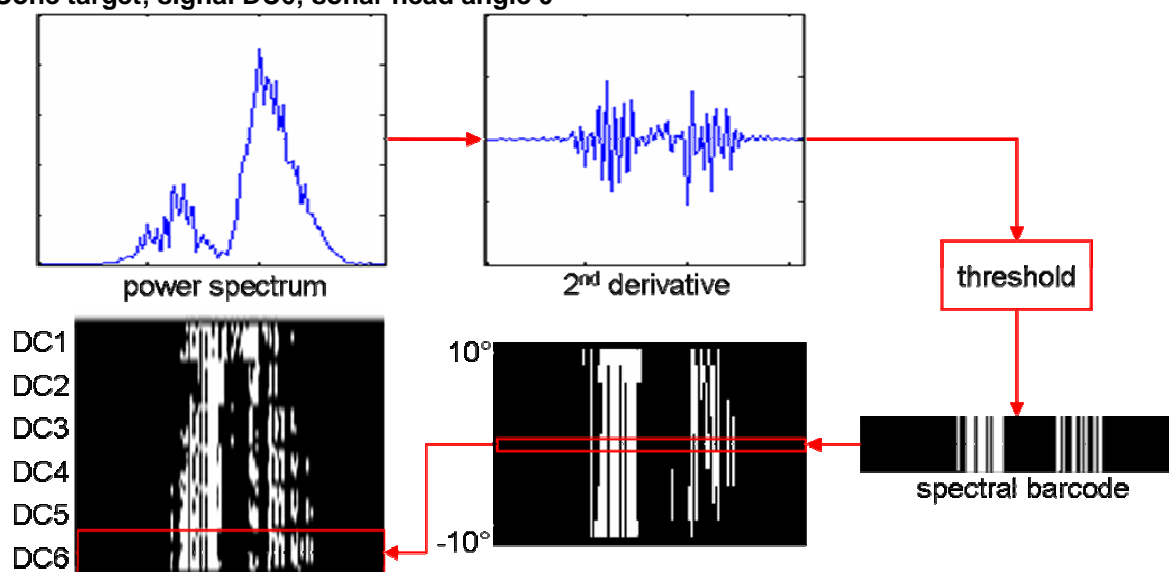


Figure 6: Formation of spectral barcode signatures from 2nd derivatives of power spectrum

Eleven echoes have been recorded for each pulse target combination investigated, with the sonar head scanning across the targets in the range  $-10^\circ$  to  $10^\circ$  in  $2^\circ$  steps. The resultant spectral barcodes are stacked into a binary image containing all 66 barcode responses for that target. Figure 5 shows eight images for a range of targets.

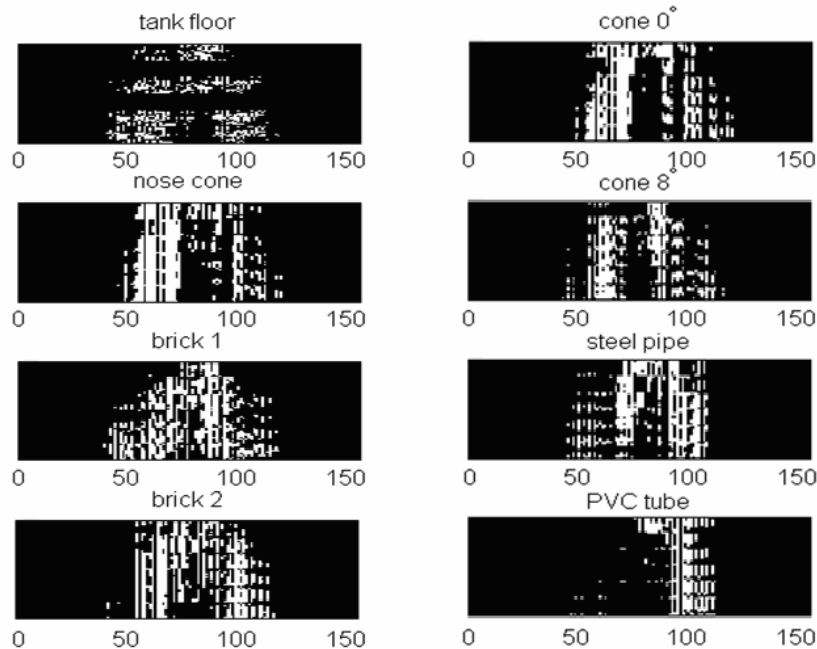


Figure 7: spectral barcodes for seven bottom-set targets – 66 responses are encoded for each target corresponding to the six transmit pulses and eleven head angles used, horizontal scale is frequency in kHz

The targets used were a small aluminium nosecone (8cm diameter), the large metallic concave cone seen in Figure 3 ensconced in two orientations (vertical and tilted  $8^\circ$  towards the sonar), a housebrick lying flat on the bottom in two orientations (wide face and narrow face towards the sonar), a steel pipe with outer diameter 168mm and wall thickness 13mm and a PVC pipe with outer diameter 170mm and 3mm wall thickness. The tank floor response gives a comparable reverberation return for the same region with no target present. For each target, the encoded responses are generally consistent between pulses and vary mostly at high frequencies with sonar head angle. This latter observation can be explained by the sonar beamwidth which is narrower for higher transmit frequencies. However, DC2 in particular is seen to produce a somewhat different response to the other pulses for some of these targets, notably the steel pipe and cone in its vertical orientation.

The binary representation provides a simple way to consider similarities between responses through binary subtraction, which yields a result analogous to the Manhattan distance metric  $\sum_{i,j} |x_{ij} - y_{ij}|$ . In Figure 6 the main axis ( $0^\circ$ ) responses are compared to all other responses at the remaining ten scan angles for each target. Intensity indicates degree of correspondence and the matrix is highly diagonal. In fact for these tests simple thresholding gives a 100% correct classification for each target. The variation in intensity does provide an indication of which objects have similar responses. The most notable similarities being between the different aspect cone returns and between the steel and PVC pipe returns.

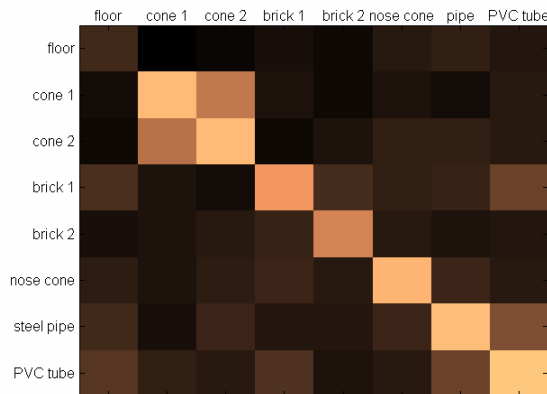


Figure 8: confusion matrix indicating similarities in response for some targets -- note that the tank floor reverberation response does not correlate well between pings

Similarities in the pipe responses are derived from their closely matched external diameters, though it is important to note that the differences are sufficient to differentiate them using their broadband echoes. These objects have target strengths within 1dB of each other and they are very difficult to distinguish in intensity images. The dual aspect concave cone returns match well indicating some robustness to target aspect. Interestingly, the two responses from the brick do not show a great degree of similarity and as might be expected multiaspect views will be required to fully characterise the response of some targets. The reverberation response seen from the floor does not correlate well between pings even for this highly structured concrete walled tank.

#### 4.3 Wavelet analysis

The simple thresholding used above is likely to suffer in a noisier environment. One approach to tackling this problem is to use a wavelet representation calculated on the echo spectra. Figure 9 illustrates the approach and shows the differences in the wavelet representation for noise and reverberation returns recorded at a harbour site on the Forth Estuary and the tube echo simulation given in Figure 4.

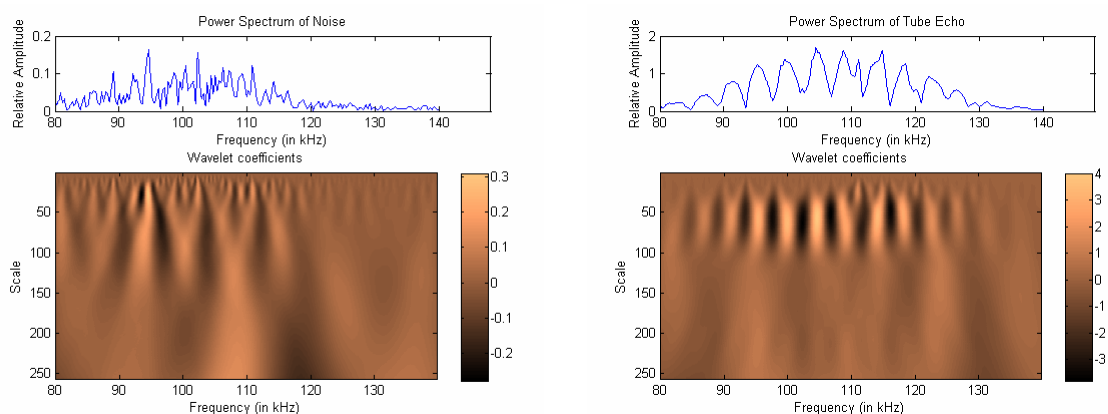


Figure 9: Power spectra and wavelet coefficients for empirical noise and theoretical spectral echo for the PVC tube

The Daubechies-5 wavelet was used and produces an effective response to the strong peak and notch features in the spectra. The noise and reverberation coefficients are strongly represented at low scale values. The target coefficients are strongest over a characteristic band at higher scales. In Figure 10 shows the equivalent wavelet representation for a simulated echo with the pipe response buried in noise at SNR=1.0, with the characteristic pipe response over scales 50-100 still dominant.

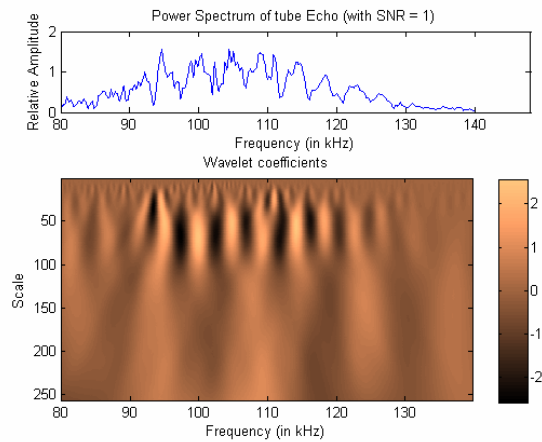


Figure 10: power spectrum and wavelet coefficients for the PVC tube echo in noise, SNR = 1.0

## ACKNOWLEDGEMENTS

This research has been supported by DSTL under the maritime countermeasures – difficult maritime targets (MCM-DMT) programme. Thanks are due to SPAWARSYSCEN, San Diego for data gathered using the DBS system under a prior ONR funded research programme.

## REFERENCES

- [1] D. Houser, S. Martin, M. Phillips, E. Bauer, T. Herrin, and P. Moore, "Signal processing applied to the dolphin-based sonar," in Proc. MTS/IEEE OCEANS 2003 San Diego, CA, pp. 297–303, 2003.
- [2] D. Houser, D. Helweg, and P. Moore, "Classification of dolphin echolocation clicks by energy and frequency distributions," J. Acoust. Soc. Am., 106, pp. 1579–1585, 1999.
- [3] W. Au, *The Sonar of Dolphins*, Springer-Verlag, New York, 1993.
- [4] C. Capus, Y. Pailhas, K. Brown and D.M. Lane, "Bio-inspired wideband sonar signals based on observations of the bottlenose dolphin (*Tursiops truncatus*)", J. Acoust. Soc. Am., 121(1), 2007.
- [5] R. Doolittle and H. Uberall, "Sound scattering by elastic cylindrical shells", J. Acoust. Soc. Am., 73, pp. 272-275, 1966.
- [6] M.I. Sanderson and J.A. Simmons, "Neural responses to overlapping FM sounds in the inferior colliculus of echolocating bats", J. Neurophysiology, 83, pp. 1840-1855, 2000.
- [7] M.I. Sanderson and J.A. Simmons, "Selectivity for echo spectral interference and delay in the auditory cortex of the big brown bat *Eptesicus fuscus*", J. Neurophysiology, 87(6), pp. 2823-2834, 2002.
- [8] J.A. Simmons, E.G. Freedman, S.B. Stevenson, L. Chen and T.J. Wohlgenant, "Clutter interference and the integration time of echoes in the echolocating bat, *Eptesicus fuscus*", J. Acoust. Soc. Am., 86(4), pp. 1318-1332, 1989.
- [9] J.M. Wotton and J.A. Simmons, "Spectral cues and perception of the vertical position of targets by the big brown bat, *Eptesicus fuscus*", J. Acoust. Soc. Am., 107(2), pp. 1034-1041, 2000.